

# 7.15 INSTANTANEOUS NEAR SURFACE AIR TEMPERATURE AND SENSIBLE HEAT FLUX FIELDS DURING THE SEMAPHORE EXPERIMENT USING SATELLITE DATA

Denis Bourras\*, Laurence Eymard†, W. Timothy Liu\*, and H el ene Dupuis\*\*

\*CALTECH, JPL, Pasadena, California, USA

†CETP/CNRS/INSU, V elizy Villacoublay, France

\*\*DGO, Universit e Bordeaux 1, France

bourras@pacific.jpl.nasa.gov

## 1 Introduction

Turbulent heat flux fields at the air-sea interface are necessary to study the upper ocean heat budget or to force ocean general circulation models (GCMs). These flux fields may be obtained mainly from atmospheric GCMs or satellite data. GCMs produce a physical and dynamical interpolation in space and time between in situ measurements. However, there are often large uncertainties in the analyses because observations are often sparse. Consequently, the analyzed horizontal atmospheric temperature and flux structures are often mislocated. Satellite data are increasingly used to retrieve the fluxes because they are geolocated and have a high temporal and spatial resolution. Although two methods have been proposed to infer the near surface air temperature ( $T_A$ ), on which the sensible heat flux ( $H_s$ ) depends, from spaceborne measurements, this is still a topic of active research (Seager et al., 1995, Jones et al. 1999).

In this paper, we propose a computationally fast physical method to obtain high spatial resolution ( $0.3 \times 0.3^\circ$ ) instantaneous  $T_A$  and sensible heat flux fields. The method is based on a horizontal temperature advection model (ADMOD). The method presented here is useful in the context of field experiments since it works on mesoscale regions ( $1000 \times 1000$  km) and uses as inputs a combination of satellite data, operational GCM analyses, and in situ measurements. The input parameters are sea surface temperature (SST) and horizontal wind vector fields,  $T_A$  around the region under study, and three constants related to humidity, mixed layer height, and temperature at the top of the mixed layer. In this paper, ADMOD is applied to European Remote Sensing Satellite (ERS-1) wind vectors, reanalyzed SST fields, and ECMWF boundary  $T_A$ . The three constants are derived from aircraft data. The method is validated using Research Vessel (R/V) in situ mea-

surements and GCM fields from the Structure des Echanges Air-Atmosphere, Proprietes des Heterogeneites Oceaniques: Recherche Experimentale experiment (SEMAPHORE). The method is described in the next section and the data sets are presented in section 3. Then, ADMOD physics is validated on GCM data (section 4). Finally,  $T_A$  and  $H_s$  are derived using satellite data during SEMAPHORE, they are compared to R/V measurements and GCM fields (section 5), and a conclusion follows (section 6).

## 2 Method

Under the assumptions of non viscous steady flow and horizontal homogeneity of turbulence, the mean potential temperature conservation equation at altitude  $z_A$  (17 m) is

$$\mathbf{u} \cdot \nabla T_A + w \frac{\partial T_A}{\partial z} = - \frac{\partial \overline{w'\theta'}}{\partial z} \quad (1)$$

where  $T_A$  is the mean potential temperature,  $\mathbf{u}$  is the horizontal wind velocity,  $w$  is the vertical wind component, and  $\overline{w'\theta'}$  is the turbulent sensible heat flux. The turbulent flux and vertical advection terms are approximated as functions of  $T_A$ , SST, and  $\mathbf{u}$ , so that the final expression of the model is written

$$\begin{aligned} \mathbf{u} \cdot \nabla T_A + [\nabla \cdot \mathbf{u} (SST - T_A)]_{w>0} + \delta \cdot z_A [\nabla \cdot \mathbf{u}]_{w<0} \\ = \frac{\alpha}{h} f(\mathbf{u}, SST, T_A, \beta_{Q_A}, \gamma_{P_S}) \end{aligned} \quad (2)$$

where  $\alpha$  is 1.2 (Tennekes, 1973),  $\gamma_{P_S}$  is 1013.5 mb,  $\beta_{Q_A}$  is  $11.3 \text{ g} \cdot \text{kg}^{-1}$  (a climatological value for the SEMAPHORE region),  $\delta$  is constant,  $h$  is the boundary layer height, which is assumed constant at the scale of the experiment, and  $f$  is a function that corresponds to a bulk flux algorithm (Bourras, 1999).

### 3 Data sets

The data used were collected during the SEMAPHORE experiment (Eymard et al., 1996), from 15 October to 15 November 1993, and from 30° to 38° N and 20° to 28° W. Three types of data are described hereafter, namely ADMOD input data, ADMOD validation data and an additional test data set.

ADMOD input wind fields are ERS-1 wind vectors at  $0.3 \times 0.3^\circ$  resolution. High resolution ( $0.16 \times 0.16^\circ$ ) SST fields are used. They are described in Giordani et al. (1998). Boundary  $T_A$  come from  $1.125 \times 1.125^\circ$  resolution operational analyses from the European Centre for Medium Range Weather Forecasting (ECMWF). The maximum time difference between SST, ECMWF, and ERS-1 fields is 16 min. The different fields are interpolated at the ERS-1 resolution.  $\delta$  and  $h$  are derived from aircraft data (e.g. Kwon et al., 1998).  $h$  is 580 m and  $\delta$  is  $0.14 \pm 0.03 \text{ K.m}^{-1}$ . Local validation data are measurements performed inboard R/V *Le Suroit*, averaged over one hour periods. Validation fields are ECMWF analyses and high resolution ( $0.16 \times 0.16^\circ$ ) reanalyses of the Action de Recherche Petite Echelle Grande Echelle (ARPEGE) model (Giordani et al., 1998). The test data consist in 32 ARPEGE reanalyses selected from 15 October to 15 November 1993, at 0600 UTC, and from 30° to 38° N and 20° to 28° W.

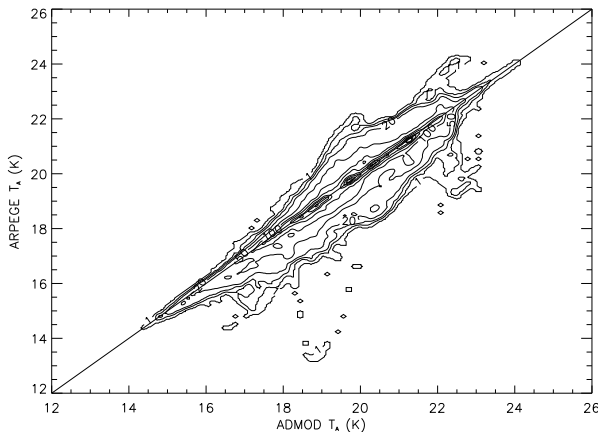


Figure 1: Comparison between ARPEGE and ADMOD  $T_A$  fields. The ARPEGE reanalyses are used to force ADMOD. Contour lines represent the density of points. Unit is in number of points per  $0.1 \text{ K} \times 0.1 \text{ K}$  area.

### 4 Validation of the method

In this section,  $\mathbf{u}$  and SST fields, and boundary  $T_A$  from GCMs are used to force ADMOD. The ADMOD  $T_A$  and  $H_s$  obtained are then compared to the original GCM  $T_A$  and  $H_s$ . GCM data are the ARPEGE reanalyses of the test data set. The study is divided in two parts: first, ADMOD is applied in cases where  $\nabla \cdot \mathbf{u}$  is negligible. Next, ADMOD error is analyzed in convergent and divergent cases.

Under horizontal advection conditions, the rms deviation between the estimated ADMOD  $T_A$  and the original ARPEGE  $T_A$  is 0.78 K. The mean difference between ADMOD and ARPEGE  $T_A$  is 0.78 K and the correlation coefficient is 0.89 (figure 1). Peak deviations are +5.1 K and -1.49 K, respectively. The correlation between individual ADMOD and ARPEGE  $T_A$  fields is always larger than 0.6 and greater than 0.8 in 15 out of 19 cases. The correlation between ADMOD and ARPEGE fluxes on all data is 0.88, the rms error is  $8.5 \text{ W.m}^{-2}$ , and the bias is  $-5.1 \text{ W.m}^{-2}$ .

$\mathbf{u}$  fields, SST fields, and boundary  $T_A$  from ARPEGE are used to force ADMOD under divergent and convergent conditions, successively. First, ADMOD is applied to  $\mathbf{u}$ , SST, and boundary  $T_A$  from ARPEGE in 10 anticyclonic cases. The VAP enhances ADMOD results only beyond  $\nabla \cdot \mathbf{u} = 3.5 \times 10^{-5} \text{ s}^{-1}$ . Beyond this threshold, the correlation between ARPEGE and ADMOD  $T_A$  fields is 0.73, the rms deviation is 1.13 K, and there is no bias. If the VAP is not implemented into ADMOD, then the rms becomes 1.23 K, a bias appears (0.8 K), and the correlation drops to 0.5. In convergent cases, the VAP has a slightly negative impact on the results. The rms deviation is increased by 0.1 K if the VAP is implemented into ADMOD. A more complicated parametrisation needs to be developed in this case.

### 5 Application of ADMOD to SEMAPHORE data

In this section, ADMOD is run on the application data set. The estimates of  $T_A$  and  $H_s$  are successively compared to validation data.

Comparison between in situ  $T_A$  and ADMOD  $T_A$  are shown in Figure 2. The rms deviation between ADMOD and the R/V is 0.77 K, which is comparable to the error obtained in section 4. The correlation coefficient is 0.87 and the bias 0.93 K. The R/V data have a better fit to ECMWF than ADMOD or ARPEGE, which temperatures are close. In figure 2, four points corresponding to 19 October are strongly biased for ADMOD and the two GCMs, by 2 K. We

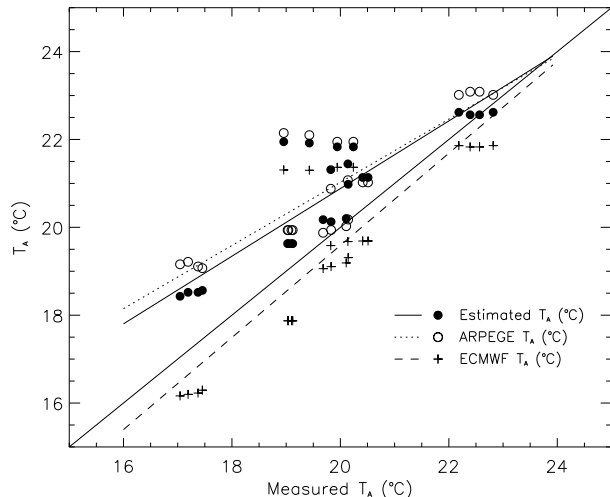


Figure 2: Validation of ADMOD  $T_A$  estimates. R/V measurements (x-axis) are compared to ADMOD (dots), ARPEGE (circle), and ECMWF (crosses)  $T_A$ .

consider that these points are bad R/V measurements since there is no noticeable discrepancy between the R/V and ADMOD in terms of wind speed and SST for that time. R/V and ADMOD fluxes compare well except for the four underestimated points described above. They correspond to positive R/V and negative ECMWF, ADMOD, and ARPEGE fluxes. If these four points are omitted, the correlation coefficient between the R/V and ADMOD  $H_s$  is 0.7, the rms deviation is  $-5.5 \text{ W.m}^{-2}$ , and the bias is  $-8.5 \text{ W.m}^{-2}$ .

## 6 Conclusion

An original method to derive mesoscale sensible heat flux fields from satellite data, in situ measurements, and GCM operational analyses is proposed. The method is based on an advection temperature model. In the context of a field experiment GCM operational analyses are often the only available source to obtain  $T_A$  and  $H_s$  fields. The method proposed may help to enhance these fields in resolution and accuracy in the context of a field experiment. Plus, the method is computationally fast to run, as opposed to the heavy process which consists in assimilating satellite data in GCMs. The fields produced by this method were found consistent with fields from two GCMs on the SEMAPHORE region. The intrinsic rms error of the method is 0.8 K for  $T_A$  and  $10 \text{ W.m}^{-2}$  for  $H_s$ . The method was applied to ERS-1 wind vectors, high resolution SST fields and ECMWF  $T_A$  conditions. The comparison between the  $T_A$  and  $H_s$  retrievals and

R/V data gave the following rms errors: 0.8 K and  $10 \text{ W.m}^{-2}$ , which is encouraging since it exactly corresponds to the intrinsic error of the method.

## Acknowledgements

This study was performed, in part at the Jet Propulsion Laboratory, California Institute of Technology, under contract with National Aeronautics and Space Administration (NASA). It was partly supported by the Physical Oceanography Program of NASA. This work was also performed under contract with French Direction Générale de l'armement, Direction de la Recherche et de la Technologie, and French Centre National de la Recherche Scientifique (CNRS).

## References

- [1] Bourras, D., 1999: Estimation of the latent heat flux over oceans from satellite data, Thesis, 203 pp., Paris VI University, France.
- [2] Eymard, L., S. Planton, P. Durand, C. Le Visage, P. Y. Le Traon, L. Prieur, A. Weill, D. Hauser, J. Rolland, J. Pelon, F. Baudin, B. Bénéch, J. L. Bringuier, G. Caniaux, P. De Mey, E. Dombrowski, A. Druilhet, H. Dupuis, B. Ferret, C. Flamant, F. Hernandez, D. Jourdan, K. Katsaros, D. Lambert, J. M. Levfevre, P. Le Borgne, B. Le Squere, A. Marsoin, H. Roquet, J. Tournadre, V. Trouillet, A. Tychensky, B. Zakardjian, 1996: Study of the air-sea interactions at the mesoscale: The SEMAPHORE experiment, *Ann. Geophysicae*, **14**, 986-1015.
- [3] Kwon B. H., B. Bénéch, D. Lambert, P. Durand, A. Druilhet, H. Giordani, and S. Planton, 1998: Structure of the marine atmospheric boundary layer over an oceanic thermal front: SEMAPHORE experiment, *J. Geophys. Res.*, **103**, C11, 25159-25180.
- [4] Giordani, H., S. Planton, B. Bénéch, and B.H. Kwon, 1998: Atmospheric Boundary Layer Response to Sea Surface Temperatures during the SEMAPHORE Experiment, *J. Geophys. Res.*, **103**, C11, 25,047-25,060.
- [5] Jones C., P. Peterson, and C. Gautier, 1999: A new satellite method for deriving ocean surface specific humidity and air temperature: An artificial neural network approach, *J. Appl. Meteor.*, **38**, 1229-1245.
- [6] Seager, R., M. B. Blumenthal, and Y. Kushnir, 1995: An advective Atmospheric Mixed Layer

Model for Ocean Modeling Purposes: Global Simulation of Surface Heat Fluxes, *J. Climate*, **8**, 1951-1964.

- [7] Tennekes, H., 1973: The logarithmic wind profile, *J. Atmos. Sci.*, **30**, 234-238.